



Influence of Precipitation Behavior of (Ti, Mo)C Carbides on the Microstructure and Mechanical Properties of Medium Manganese Steels

D. F. Xu^{1,2}, S. H. Sun^{1,2}, and M. H. Cai^{1,3}(✉)

¹ School of Materials Science and Engineering, Northeastern University, Shenyang 110819, China

caimh@smm.neu.edu.cn

² Key Lab of Lightweight Structural Materials, Northeastern University, Shenyang 110819, China

³ State Key Lab of Rolling and Automation, Northeastern University, Shenyang 110819, China

Abstract. Although the medium manganese steel has a high value of the product of tensile strength and elongation, it has the disadvantage of low yield strength. To solve this problem, two Fe-Mn-Al-C steels with (Ti, Mo) and without (Ti, Mo) were designed to analyze the effect of microalloy elements on their microstructure and mechanical properties. The steels were annealed at different temperatures for 24 h to obtain a stable microstructure close to equilibrium. The addition of Ti-Mo increased the yield strength by 150–300 MPa, and the maximum increment in yield strength was achieved at an intercritical annealing temperature of about 610 °C. The increase in yield strength is mainly attributed to grain refinement and precipitation hardening with the addition of Ti-Mo.

Keywords: Medium manganese steel · Microalloying · Precipitation kinetics · Microstructural evolution · Mechanical properties

1 Introduction

Medium manganese steel has received considerable attention as a third-generation advanced automotive steel because of its excellent properties that are expected to meet the requirements of the automotive manufacturing industry. However, intercritical annealing usually softens the matrix and sharply decreases the yield strength [1–3], while the addition of microalloy elements can effectively improve the matrix strength through mechanisms such as precipitation strengthening and grain refinement [4]. In particular, the combination of Mo and other microalloying elements can significantly increase the precipitation density and reduce the carbide particle size. Ti is less expensive and has a high precipitation potential, and Lee et al. reported that Ti-Mo additions to Mn steels can improve strength without loss of elongation [5]. However, the precipitation behavior of Ti-Mo composite additions in medium Mn steels and their effects on microstructure and mechanical properties need further investigation.

In this work, Fe-0.2C-6Mn steel with (Ti, Mo) and without (Ti, Mo) was annealed at different temperatures for 24 h to obtain a stable structure close to equilibrium, to analyze the effect of microalloying on the microstructure evolution and carbide precipitation behavior.

2 Materials and Experimental Procedures

Two medium manganese steels with different compositions (Fe-6Mn-0.2C-1Al and Fe-6Mn-0.2C-1Al-0.08Ti-0.22Mo). The forged billets were heated at 1250 °C for 2 h, rolled into 5 mm thick steel plates, and air-cooled to room temperature. The steel plate was heated to 630 °C and warm rolled into a 1.4 mm thick strip. Specimens were annealed at 610 °C and 650 °C for 24 h and then air-cooled to room temperature.

The tensile test was performed at a strain rate of $5 \times 10^{-3} \text{ s}^{-1}$. Microstructural characterization was performed using field-emission scanning electron microscopy and scanning transmission electron microscopy.

3 Results

3.1 Mechanical Properties

As shown in Fig. 1, the yield strength (YS) of both steels showed a significant decreasing trend as the IA temperature increased from 610 °C to 650 °C, and the total elongation showed the opposite trend. The increase in yield strength after annealing at 610 °C reached a maximum value of about 305 MPa for the steel containing (Ti, Mo) compared to the steel without (Ti, Mo).

3.2 Microstructures Characterization

The effects of microalloying elements and temperature on the evolution of microstructure were investigated by EBSD as shown in Fig. 2. The matrix structure of the samples without (Ti, Mo) underwent sufficient recovery and recrystallization, showing an equiaxed shape, but the addition of microalloying elements significantly inhibited the dislocation recovery, and some slate-like structures with a selective orientation along the rolling direction and finer organization appeared in the samples contained (Ti, Mo).

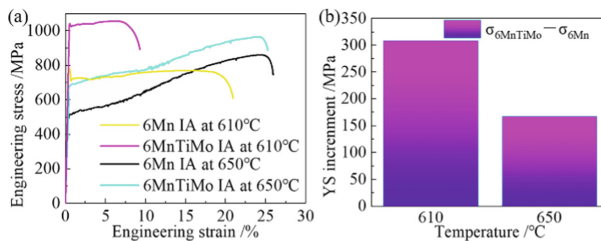


Fig. 1. The engineering tensile stress-strain curves of the steels treated at 610, 650 °C for 24 h (a) and YS increment.

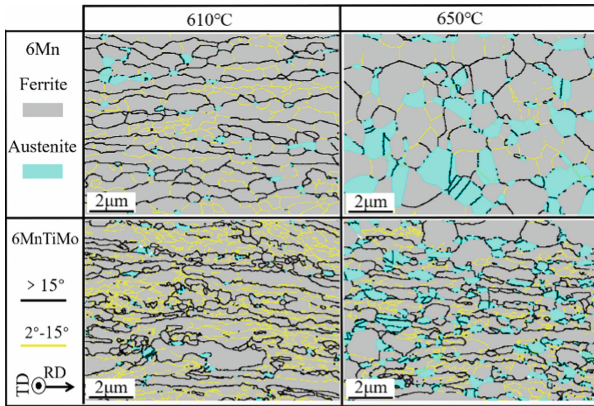


Fig. 2. EBSD phase diagrams of two steels treated at 610 °C and 650 °C for 24 h.

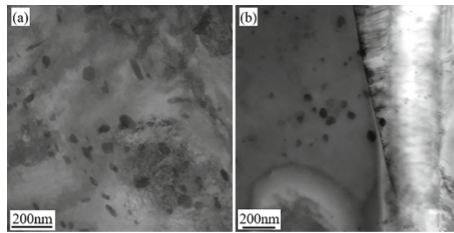


Fig. 3. The TEM micrographs of the Ti-Mo-containing steel are treated at 610 °C (a) and 650 °C (b).

Table 1. The grain size (\bar{d}), the precipitates size (d^*), and the precipitation volume fraction of the steels.

Temperature/°C	$\bar{d}/\mu\text{m}$		d^*/nm	f
	6Mn	6MnTiMo	6MnTiMo	6MnTiMo
610	1.2	1.0	13.5	2.7×10^{-2}
650	2.2	2.0	17	1.3×10^{-2}

3.3 Precipitation Characteristic

The precipitation behavior of Ti-Mo-containing steel after heat treatment at 610 °C and 650 °C for 24 h is shown in Fig. 3. The (Ti, Mo)C precipitates are mainly distributed in the ferrite matrix with an average size of less than 20 nm. Table 1 quantifies the effect of temperature on precipitate size. As the treatment temperature increases, the average precipitate size increases from 13.5 nm to 17 nm, while the precipitate volume fraction shows an opposite trend.

4 Discussion

4.1 Precipitation Behavior of $(\text{Ti}_x\text{Mo}_{1-x})\text{C}$ on the Annealing Temperature

Based on the Johnson-Mehl-Avrami equation, the PTT and NrT diagram can then be plotted based on the results calculated by the following equation [6–8]:

$$\lg \frac{t^{0.05}}{t_0} = \frac{1}{n} (-1.28994 - 2 \lg d^* + \frac{1}{\ln 10} \times \frac{\Delta G + \frac{5}{3}Q}{kT}) \quad (1)$$

$$\lg(I/K)d = \lg(\pi \rho b^2 d_d^*) - \frac{(\Delta G_d^* + \frac{2}{3}Q)}{kT \ln 10} \quad (2)$$

where, d^* is critical nucleation size, ΔG is critical nucleation energy, Q is the diffusion activation energy within the crystal, k is a constant. ρ is the density of the matrix.

The PPT and NrT curves of the $(\text{Ti}_x\text{Mo}_{1-x})\text{C}$ phase are shown in Fig. 4, which indicates that nose temperatures close to 610 °C and maximum nucleation rate temperatures in the range of 550–600 °C. The composite addition of Ti-Mo increased the density of nano precipitates. The results calculated using the Avrami equation are in good agreement with the experimental observations.

4.2 Yield Strength Contribution Mechanism

The incorporation pass of Ti-Mo can be calculated by the following equation [9]:

$$\sigma = \sigma_0 + \sigma_s + \sigma_g + \sigma_p + \sigma_d \quad (3)$$

σ_0 is the ferrite friction stress (~48 MPa). σ_s , σ_g , σ_p and σ_d are the strengthening contribution caused by solid solution, grain refinement, precipitation hardening, and dislocation hardening, respectively.

The theoretically calculated values of YS are shown in Fig. 5, which are in good agreement with the experimental results. The addition of Ti-Mo improves YS mainly through grain refinement and precipitation hardening.

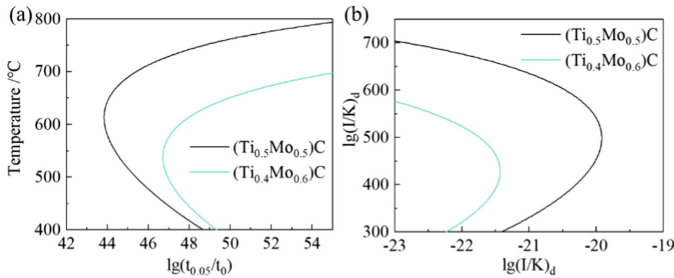


Fig. 4. The precipitation-temperature-time (PTT) curves (a), and the NrT curves of precipitation in ferrite (b).

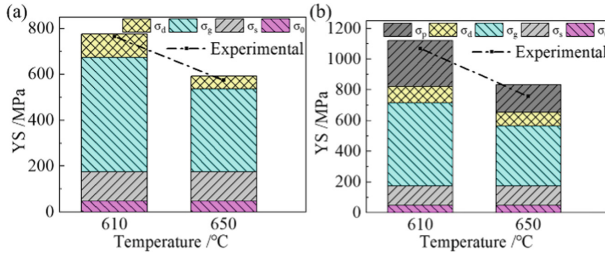


Fig. 5. The quantification of solid solution strengthening, grain refinement strengthening, dislocation hardening, and precipitation hardening of the steels 6Mn (a), and 6MnTiMo (b).

5 Conclusions

The addition of Ti and Mo can effectively improve the strength of the medium Mn steel, precipitating carbides with sizes below 20 nm in the matrix with a slight loss of plasticity, with the smallest maximum precipitation density and size at 610 °C intercritical annealings and a maximum yield strength increment of 300 MPa.

Acknowledgments. The authors gratefully acknowledge the financial support of the Natural Science Foundation of China (No. 51671149) and the Fundamental Research Funding of the Central Universities, China (Nos. N2002002/N180702012). Special thanks are due to the instrumental/data analysis from the Analytical and Testing Center, Northeastern University.

References

1. W. Q. Cao, C. Wang, J. Shi, M. Q. Wang, W. J. Hui and H Dong, Microstructure and mechanical properties of Fe-0.2C-5Mn steel processed by ART-annealing, *Mater. Sci. Eng. A* **528**, 6661 (2011).
2. B. B. He, B. M. Huang, S. H. He, Y. Qi, H. W. Wen and M. X. Huang, Increasing yield strength of medium Mn steel by engineering multiple strengthening defects, *Mater. Sci. Eng. A* **724**, 11 (2018).
3. H. Luo and H Dong, A new ultrahigh-strength Mn-alloyed TRIP steels with improved formability manufactured by intercritical annealing, *Mater. Sci. Eng. A* **626**, 207 (2015).
4. H. J. Pan, H. Ding and M. H. Cai, Microstructural evolution and precipitation behavior of the warm-rolled medium Mn steels containing Nb or Nb-Mo during intercritical annealing, *Mater. Sci. Eng. A* **736**, 375 (2018).
5. D. Lee, J. K. Kim, S. Lee, K. Lee and B. C. D. Cooman, Microstructures and mechanical properties of Ti and Mo micro-alloyed medium Mn steel, *Mater. Sci. Eng. A* **706**, 1 (2017).
6. K. Zhang, X. Sun, M. Zhang, Z. D. Li, X. Y. Ye, Z. Zhu, Z. Huang and Q. Yong, Kinetics of (Ti, V, Mo)C precipitated in γ/α matrix of Ti-V-Mo complex microalloyed steel, *Acta. Metall.* **54**, 1122 (2018).
7. H. J. Pan, H. Ding, M. H. Cai, K. Dilay and W. W. Song, Precipitation behavior and austenite stability of Nb or Nb-Mo micro-alloyed warm-rolled medium-Mn steels, *Mater. Sci. Eng. A* **766**, 138371 (2019).

8. J. H. Jang, C. H. Lee, Y. U. Heo and D. W. Suh, Stability of (Ti, M)C (M=Nb, V, Mo and W) carbide in steels using first-principles calculations, *Acta. Mater.* **60**, 208 (2012).
9. D. B. Park, M. Y. Huh, J. H. Shim, J. Y. Suh and W. S. Jung, Strengthening mechanism of hot rolled Ti and Nb microalloyed HSLA steels containing Mo and W with various coiling temperature, *Mater. Sci. Eng. A* **560**, 528 (2013).

Open Access This chapter is licensed under the terms of the Creative Commons Attribution-NonCommercial 4.0 International License (<http://creativecommons.org/licenses/by-nc/4.0/>), which permits any noncommercial use, sharing, adaptation, distribution and reproduction in any medium or format, as long as you give appropriate credit to the original author(s) and the source, provide a link to the Creative Commons license and indicate if changes were made.

The images or other third party material in this chapter are included in the chapter's Creative Commons license, unless indicated otherwise in a credit line to the material. If material is not included in the chapter's Creative Commons license and your intended use is not permitted by statutory regulation or exceeds the permitted use, you will need to obtain permission directly from the copyright holder.

